PAPER

Check for updates

Self-assembly of supra-amphiphiles building block fabricated by β-cyclodextrin and adamantane-based ionic liquid†

Xing Zhong,[a] Caixia Hu, [ID] *[a] Xiaowei Yan,*[b] Dongjian Zhu, [ID] [b] Qiujuan Chen,[b] Wenxue Li,[b] Lizhen Feng[b] and Yan Wei[b]

A new adamantane-based ionic liquid, (11-(((-adamantane-1-carbonyl)oxy)undecyl)-1-methylimidazol-3-ium bromide (AD-C$_{11}$im), was synthesized from 1-adamantanecarboxylic acid and observed that it can aggregate into micelles in aqueous solution. A number of experiments were conducted to understand the self-assembly of supra-amphiphiles building block fabricated by β-cyclodextrin (β-CD) and adamantane-based ionic liquid at diverse molar ratios. Studies revealed that host–guest interaction between the adamantane group and β-CD occurred and AD-C$_{11}$im@1β-CD building block formed when same amount β-CD was added. Then the micelles aggregates formed by AD-C$_{11}$im only turned into spherical vesicles, which was confirmed by AFM, DLS and TEM. Besides, according to the results of AFM, it can be confirmed that the vesicles were monolayer structure. When double amount β-CD was added, both the adamantane group and the hydrophobic chain were encapsulated by β-CD and AD-C$_{11}$im@2β-CD building block formed. Thus the aggregations changed from vesicles to net-like nanofiber, which was observed by TEM. When the β-CD concentration increased to 40 mM, the formation of light blue hydrogel was observed during the self-assembling process of AD-C$_{11}$im@2β-CD building block.

Introduction

Ionic liquids (ILs), which are composed of various ions, have successfully aroused the interest of many scientists during the past few years.[1] Compared with traditional organic solvents, ILs have many unique properties and are widely used in catalysis and chemosynthesis,[2,3] materials, medicine, energy applications,[4,5] carbon dioxide capture,[3,6] analytical applications,[7] and so on. ILs have been the frontier and hotspots of international green chemistry and chemical industry. Thus, it can provide new ideas to find green medium for chemist and new functional materials for materials scientists.

Recently, supra-amphiphiles serve as building block are fabricated by non-covalent interactions have been developed.[8] Host–guest interaction, especially based on cyclodextrins (CDs) is an important driving force for super-amphiphilic molecules. It is widely known that CDs are natural molecules and possess a truncated doughnut-shaped structure having hydrophobic inner cavity and hydrophilic surface.[9] The unique structure of

cyclodextrin results in accommodation of various guest molecules giving rise to the formation of inclusion complexes and these CDs inclusion have been extensively used in separation, analysis, medicine, catalysis and other fields.[10]

Both ILs and CDs have special structures and properties and exhibit excellent properties in many areas, such as synthetize, catalysis, separating process and so on. Therefore, the researches on combinations of ILs and CDs are attracting more and more attention. For examples, Amajjahe *et al.* found that [bvim][Tf$_2$N] exhibited lower critical solution temperature after adding CD and noncomplexed polymer precipitation appeared at higher temperature.[11] Han *et al.* studied the inclusion compound of β-CD and bmimPF$_6$ and discovered that the compound had higher solubility, lower thermal stability and lower decomposition temperature.[12] And they also studied the inclusion complexes of three types of ILs surfactants (C$_{12}$-mimPF$_6$, C$_{14}$mimPF$_6$ and C$_{16}$mimPF$_6$) with β-CD, found the inclusion compound exhibited a channel-type structure and announced the importance of hydrophobicity during the process.[13] Schmitzer *et al.* used [C$_{12}$MIM]/[C$_{16}$MIM] and CD combination for the rhodium-catalyzed hydroformylation reaction of alkenes which not dissolved in water and this created high activity, high regioselectivity and decreased decantation time. This group also demonstrated that the supramolecular compounds formed by CDs and imidazolium salts can be used to alter the first- and the second-coordination sphere of an organometallic predecessor.[14] Roy *et al.* explored inclusion compounds of ILs, 1-butyl-4-methylpyridinium lauryl

[a]*State Key Laboratory for Nuclear Resources and Environment, School of Chemistry, Biology and Materials Science, East China University of Technology, Nanchang, 330013, China. E-mail: hezhou8@foxmail.com*

[b]*Guangxi Key Laboratory of Calcium Carbonate Resources Comprehensive Utilization, College of Materials and Environmental Engineering, Hezhou University, Hezhou 542899, China. E-mail: yanxiaoweizb@163.com*

sulfate, with β-CD and revealed the unparalleled configuration of the inclusion compound and they found the concurrence of micelle and vesicle.[15] Shen *et al.* suggested a universal interaction between an IL (C$_{12}$mimBr) and β-CD and confirmed that imidazolium ring didn't come into the β-CD cavity.[16] What' more, they also found that vesicle was formed in the system and the vesicle will become lamellae hydrogel if lower the temperature, which is reversible and reproducible.[17] In short, ILs and CDs can form inclusion complexes by host–guest interactions. However, all of these are about the formation and mechanism of ILs and CDs inclusion complexes, or the changes of physicochemical properties of ILs system by adding cyclodextrins. Self-assembly of adamantane-based ionic liquid by adding CDs at different molar ratios were seldom discussed.

Adamantane is a symmetric tricyclic hydrocarbon composed of 10 carbon atoms and 16 hydrogen atoms,[18–20] and it was a classic guest molecular for β-CD owing to its high association constants. In this work, a cationic adamantane-based ionic liquid, AD-C$_{11}$im (the chemical structure shown in Fig. 1), has been synthesized from 1-adamantanecarboxylic acid. The synthesis route is illustrated in the ESI (Scheme S1†). Thus, the AD-C$_{11}$im molecular can provide two binding sites for β-CD: one is alkane chain; the other is adamantane.[21,22] Different binding sites may lead to form different building blocks due to host–guest interaction, and then form diverse aggregate morphology. Hence, it will be very interesting to investigate the binding sites of AD-C$_{11}$im and the aggregate morphology transformation by adding β-CD at different molar ratios. For better understanding the effects on the aggregate morphology of AD-C$_{11}$im by adding β-CD the host–guest inclusion compounds formed by AD-C$_{11}$im and β-CD at diverse molar ratios were discussed.

Experimental

Materials and apparatus

The synthetic process and treatment of 11-bromoundecyl adamantane-1-carboxylate are mentioned in our previous article.[20] 11-Bromo-1-undecanol, *p*-toluenesulfonic acid monohydrate, 1-methylimidazole, β-cyclodextrin were acquired from Energy Chemical and used as received. Reagent grade materials were prepared. High-purity water (18.25 MΩ cm) was used to prepare all aqueous solutions.

^{1}H NMR, ^{13}C NMR and ^{1}H–^{1}H 2D ROESY NMR measurements were performed on Bruker Avance-400 spectrometer operating at 400 MHz. ESI-MS was carried out on a mass spectrometer (6120 Single Quad, Agilent). Electrical conductivity of samples was performed on conductivity meter at 25 °C (DDS-307A, Rex Shanghai). Moisture should be removed prior to FT-IR measurements (Spectrum Two, PerkinElmer).

Samples preparation

The samples were prepared *via* mixing AD-C$_{11}$im and β-CD in proportion with 1 : 1 or 1 : 2 in aqueous solution and heated to get hyaline solutions in succession. After that, the mixtures were kept at room temperature for one day at any rate to form aggregates. The summation of AD-C$_{11}$im was used as the molar concentration of inclusion in the mixture system in the article and the AD-C$_{11}$im concentration changed from 5 to 100 mM.

Thermogravimetric (TG) tests

Thermogravimetric (TG) tests were performed on a TGA 4000 PerkinElmer instrument, each sample was heated at a rate of 10 °C min^{-1} from 50 °C to 500 °C under N$_2$ atmosphere. The inclusion complexes of AD-C$_{11}$im and β-CD were prepared by suspension method and then dried. The physical mixtures were obtained by mixing the pure of AD-C$_{11}$im and β-CD.[23]

Dynamic light scattering (DLS)

The hydrodynamic sizes of samples were determined by Zetasizer (Malvern, UK). All samples were conducted at room temperature with 633 nm laser light and the scattering angle was fixed at 90°. Before examination, the samples were filtered through a 450 nm filter.

Transmission electron microscopy (TEM)

The morphology of these samples was studied using transmission electron microscope working at 200 kV (FEI, USA). A spot of the sample was put onto a copper mesh coated with carbon, and then prepared with negative-staining. The superfluous solution was wiped away with filter paper cautiously, and the samples were then air-dried for TEM observation.

Atomic force microscopy (AFM)

AFM images were obtained using Icon scanning probe microscope (Bruker, USA). A 5 μL portion of the sample was put onto caller mica. Two minutes later, the excess aqueous solution was wiped away with filter paper carefully, and the sample-loaded mica was air-dried for AFM observation in Tapping Mode.
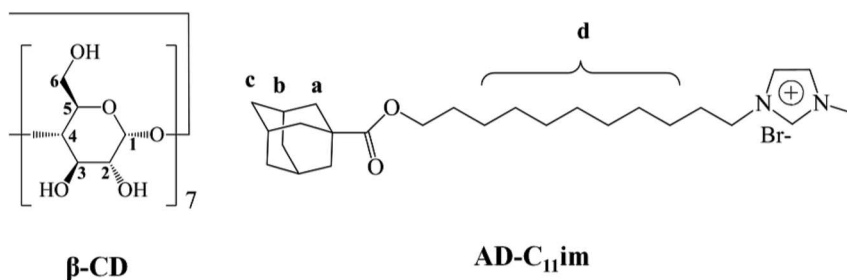

Fig. 1 Molecular structures of β-CD and AD-C$_{11}$im.

Scanning electron microscopy (SEM)

SEM was performed by field emission scanning electron microscopy (JEOL, Japan). After lyophilization in a vacuum extractor at -50 °C for 12 hour, the freeze-dried samples were cut into thin slices and stuck to the double adhesive carbon tape. The samples were sprayed a thin layer of gold before observation.

Small angle X-ray scattering (SAXS)

Small Angle X-Ray Scattering (SAXS) measurement was determined by an Anton Paar Saxesess mc2 instrument (Cu-Kα, $\lambda = 0.154$ nm). The X-ray generator was operated at 40 kV and 50 mA. The sample was measured at 25 °C.

Results and discussion

Phase diagrams of AD-C$_{11}$im/β-CD system

The AD-C$_{11}$im aggregation transformation by adding β-CD in diverse proportions were discussed in detail in this article and the appearance photos for five representative sample of AD-C$_{11}$im/β-CD system at diverse molar ratios were displayed in Fig. 2. Results showed that AD-C$_{11}$im aqueous solution maintained water-like even increasing the concentration to 200 mM without adding β-CD same as the picture in Fig. 2a, and was proved to be micelles by DLS, which were as well found in previous studies.[24,25] When β-CD was put into AD-C$_{11}$im aqueous solution at 1 : 1 molar ratio, the solution was also water-like liquid shown in Fig. 2b even the concentration of AD-C$_{11}$im increased to 80 mM, which turned out to be vesicles by DLS, TEM and AFM. Next, β-CD was added to another AD-C$_{11}$im aqueous solution at 1 : 2 molar ratios. Results showed that there were three phase states found in 1 : 2 system shown in Fig. 2c–e. The solution was transparent liquid like picture in Fig. 2c when the concentration of AD-C$_{11}$im bellowed 10 mM. Increasing the concentration of AD-C$_{11}$im (<25 mM, including 10 mM), the transparent liquid became suspension, which was proved to be net-like nanofibers by TEM. At a little higher concentration (<35 mM), the samples became non-transparent and viscoelastic (Fig. 2d), indicating the possible formation of large aggregates. Keeping the concentration increasing (≥35 mM), the samples

did not flow even by inversion of the vial, indicating the formation of hydrogel shown in Fig. 2e.

Through these above studies, micelles, vesicles, net-like nanofibers and hydrogel were spotted in AD-C$_{11}$im/β-CD system. It can be known that the aggregation behaviors of AD-C$_{11}$im can be altered by adding β-CD at different ratios. Thus, it will be very interesting to explore how aggregation behaviors happened. Certainly, studies on aggregation behaviors of the ionic liquid-type surfactant (AD-C$_{11}$im) itself should be first carried out.

Micellization of the AD-C$_{11}$im solution

AD-C$_{11}$im, a ionic liquid-type surfactant, will share the same features with traditional surfactants, for instance, micellization in aqueous solutions.[23,24] According to this, electrical conductivity (κ) was used for explaining the micellization of AD-C$_{11}$im. Results were shown in Fig. S2.† From Fig. S2,† the critical micellization concentration of AD-C$_{11}$im was about 1.8 mM. Beyond that, DLS was also used to measure the formed micelle sizes at concentrations of 5 and 10 mM, which can be found in Fig. S3a† by scattering intensity and Fig. S3b† by volume. It can be seen that the average hydrodynamic radius (Rh) of micelles were varied slightly from about 2 to 11 nm.

Because the AD-C$_{11}$im molecule has two inclusion sites which can be encapsulated by β-CD: one is the end of the adamantane group, the other is the intermediate alkyl chain of the molecule. Therefore, through adding cyclodextrin into the micelle sample step by step, AD-C$_{11}$im and β-CD can form different structural building units through host–guest inclusion, and then obtain ordered molecular aggregates with various structures. The structural information of these aggregates will be discussed in detail below.

NMR characterization for AD-C$_{11}$im/β-CD inclusions

According to the previous statement, both adamantane group and alkyl chain can be encapsulated by β-CD. To further verify this, 1D and 2D H NMR (ROESY) were performed.

1D H NMR can directly check the interaction between molecules, by observing the chemical shift of hydrogen to infer the interaction between molecules. It is well known that H-3
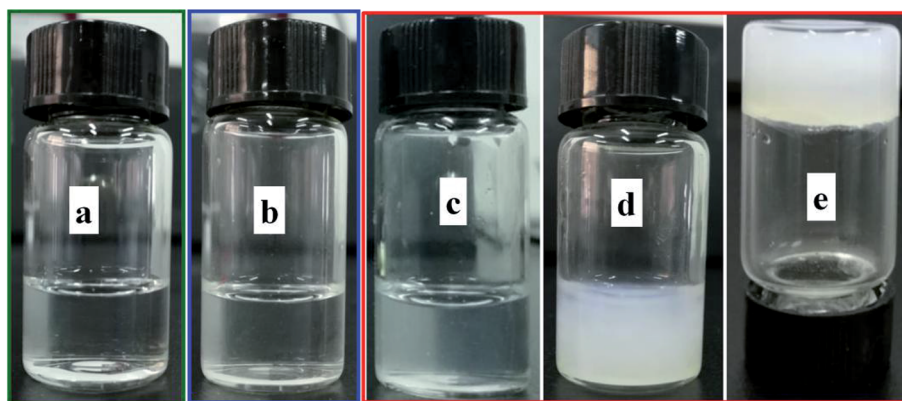

Fig. 2 Representative sample appearance images of 10 mM AD-C$_{11}$im (a), 10 mM AD-C$_{11}$im@1β-CD (b), 10 mM AD-C$_{11}$im@2β-CD (c), 25 mM AD-C$_{11}$im@2β-CD (d), and 40 mM AD-C$_{11}$im@2β-CD (e).

and H-5 are hydrons that located in the lumen of β-CD. When the guest molecule enters the cavity, the shielding effect will cause the proton chemical shifts of them.[26,27] Thus, Job's curves,[19,28] same to our previous research methods,[20] were plotted by measuring the chemical shifts of H-3 and H-5 at different concentration ratios to check the maximum stoichiometry of AD-C_{11}im/β-CD system, which were shown in Fig. 3. From Fig. 3, when $r = 0.67$, the Job's curves of both H-3 and H-5 obtained the peak, which meant that the molar ratio of AD-C_{11}im/β-CD system was 1 : 2, that is to say, one AD-C_{11}im can combine with not more than two cyclodextrins.

It has been proved that the maximum stoichiometry of AD-C_{11}im/β-CD system was 1 : 2. According to the literature data, the adamantane can combine with β-CD and the binding constant is 10^5 M^{-1},[26,29,30] which is stronger than that of alkyl chain (almost 10^3 M^{-1}) in aqueous solution.[22,31,32] Thus, it will be very interesting to explore the inclusion site of β-CD at different molar ratios.

As is known to all, hydrophobic chain is quite important for foaming capacity of surfactants. Hence, foaming ability and foam stability can indirectly reflect whether the hydrophobic chain is encapsulated by β-CD.[33] Once the alkyl chain enters into the β-CD cavity, the foam formed by surfactant would be destroyed. In order to confirm this, a control test of foamability in different system was launched. Photos in Fig. 4 reflected that a lot of foams were appeared when the system was AD-C_{11}im itself or a 1 : 1 system, indicating the alkyl chain was not encapsulated by β-CD when the molar ratio was 1 : 1. At the same time, the foam vanished quickly when the molar ratio was 1 : 2. It states the hydrophobic chain was encapsulated by β-CD. Furthermore, to confirm the formation of AD-C_{11}im@2β-CD inclusion complexes, the thermogravimetric (TG) tests were performed. Results were exhibited in Fig. S4.† As shown in Fig. S4,† the TG patterned illustrated that pure AD-C_{11}im and β-CD decomposed at about 85 and 301 °C, separately. Compared the TG curve of AD-C_{11}im/β-CD inclusion complexes with physical mixtures, it is not difficult to find that the inclusion complexes possessed high decomposition temperature, which implies that the AD-C_{11}im@2β-CD host–guest inclusion complexes were indeed formed.
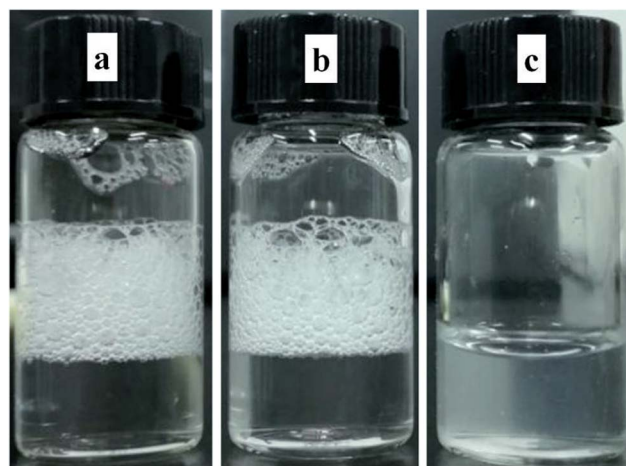

Fig. 4 Foam generated by 10 mM AD-C_{11}im (a), 10 mM AD-C_{11}im@1β-CD (b), and 10 mM AD-C_{11}im@2β-CD (c).

^{1}H–^{1}H 2D ROESY NMR, which can reflect the interaction between hydrogen atoms with space distance less than 0.5 nm, is an effective way to study host–guest inclusion interaction. In order to confirm the formation of inclusion complexes between AD-C_{11}im and β-CD at different molar ratios, 2D ROESY spectra of AD-C_{11}im/β-CD inclusions in proportion of 1 : 1 and 1 : 2 were performed and data were exhibited in Fig. 5. As shown in Fig. 5a, correlation signals of H-3 and H-5 in β-CD molecular with methylene and tertiary hydrogen in adamantane were detected (marked by squares). Nevertheless, the correlations between H-3 and H-5 and alkyl chain were not found. Simultaneously, Fig. 5b revealed that correlation signals of H-3 and H-5 with adamantane group (marked by squares) and alkyl chain (marked by circles) were both tested. Based on these data, it can be concluded that just adamantane group was encapsulated by β-CD and the alkyl chain in the molecule was not encapsulated in a 1 : 1 system, thus forming the inclusion compound AD-C_{11}im@1β-CD. Furthermore, both adamantane group and alkyl chain were encapsulated by β-CD in a 1 : 2 system, forming the inclusion compound AD-C_{11}im@2β-CD.
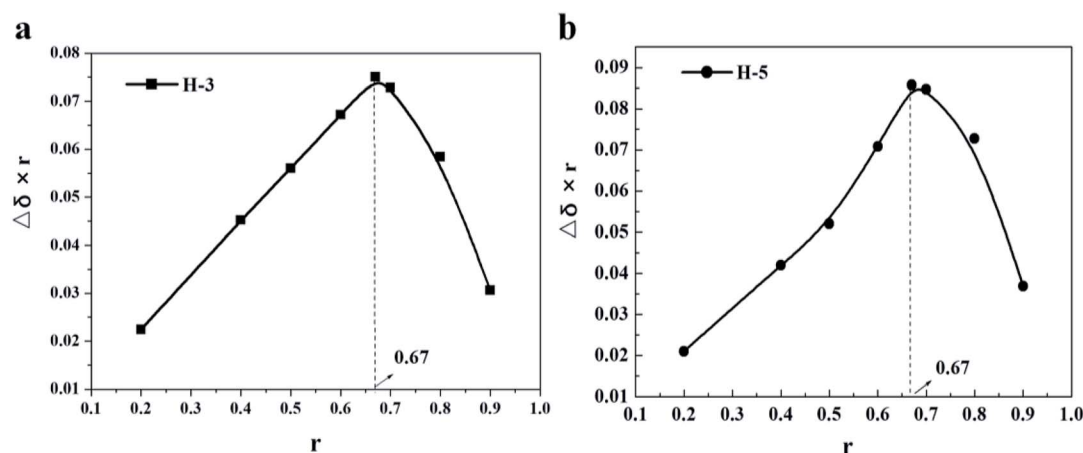

Fig. 3 ^{1}H NMR Job's curves base on H-3 (a), and H-5 (b) of β-CD in D$_2$O.

Fig. 5 ^{1}H–^{1}H 2D ROESY spectra of 10 mM AD-C$_{11}$im@1β-CD (a) and 10 mM AD-C$_{11}$im@2β-CD (b).

Self-assembling behaviors of AD-C$_{11}$im@1β-CD

Inclusion compound AD-C$_{11}$im@1β-CD, which was obtained by adding β-CD into AD-C$_{11}$im aqueous solution at a molar ratio of 1 : 1, can be regarded as an asymmetric bola amphiphilic molecule with imidazole and β-CD as the head group. To investigate micelle aggregates formed by AD-C$_{11}$im when adding the same amount β-CD, DLS were employed for AD-C$_{11}$im@1β-CD at 10 mM (shown in Fig. 6a by scattering intensity and Fig. S5† by volume). Compared with the DLS results for AD-C$_{11}$im, the average hydrodynamic radius (Rh) values of 10 mM AD-C$_{11}$im@1β-CD inclusion were about 186 nm and 164 nm by scattering intensity and volume, respectively. The AD-C$_{11}$im@1β-CD inclusion was much larger than AD-C$_{11}$im at the some concentration. This suggested the formation of new aggregation different from the micelles formed by AD-C$_{11}$im itself. To make clear the morphology of the new aggregation, the negative-staining TEM of AD-C$_{11}$im@1β-CD at 10 mM was tested and pictures were exhibited in Fig. 6b and c. The result of TEM illustrated that spherical vesicles (marked with pink arrows in Fig. 6b), the diameter of which varied from 60 to 110 nm, formed after adding β-CD into AD-C$_{11}$im aqueous solution at a molar ratio of 1 : 1. The diameter of TEM was smaller than that of DLS and it may be the result of drying process before TEM measurement. What's more, the polygonal aggregates proved to be formed by β-CD were observed in Fig. 6b (marked with yellow dashed arrow).[19]

In order to confirm the arrangement of AD-C$_{11}$im@1β-CD in the vesicle structure, AFM was measured and results were shown in Fig. 7. Vesicle structure, similar to TEM, was found from AFM results shown in Fig. 7a and diameters of these spherical aggregates arranged from 60 nm to 110 nm, which was same with TEM results. Two spherical aggregates were selected to investigate the thickness of vesicle wall and the heights (shown in Fig. 7b) were 5.88 nm and 5.41 nm, separately. It can be concluded that the average wall thickness of

these vesicles was around 2.82 nm basically equivalent to the size of AD-C$_{11}$im@1β-CD (2.85 nm) calculated according to the Corey–Pauling–Koltun (CPK) model shown in Fig. 7c. Therefore, the conclusion that AD-C$_{11}$im@1β-CD molecules are arranged in a single layer in the vesicle wall rather than in a double layer can be drawn from the results described above.[19]

As an asymmetric bola amphiphilic molecule with two head group, one of them has positive charge (the imidazole ring) and the other has no charge (β-CD). Thus, the zeta potential (ζ) measurement may be useful to make a thorough inquiry about how the AD-C$_{11}$im@1β-CD molecules arrayed in the vesicle wall.[34,35] Due to AD-C$_{11}$im containing an imidazole group with positive charge, the zeta potential value of micelles formed by AD-C$_{11}$im only was +32.3 mV in aqueous solution when the concentration was 10 mM. However, the ζ value of vesicles formed by AD-C$_{11}$im@1β-CD at 10 mM was just +10.4 mV, which was much smaller than that of AD-C$_{11}$im. It means that a majority of these asymmetric bola amphiphilic molecules existed in the arrangement of the non-charged large-head cyclodextrin group in the outer wall and the charged pyridine group in the inner wall and formed single-layer vesicle, which was asymmetrical in the inner and outer surfaces.

Self-assembling behavior of AD-C$_{11}$im @2β-CD

β-CD was added to the vesicle formed by AD-C$_{11}$im@1β-CD until the molar ratio of AD-C$_{11}$im: CD was 1 : 2 and superfluous β-CD would be combined with the alkyl chain. In the light of the literature and the above findings, it can be considered that the great majority of alkyl chains in AD-C$_{11}$im molecular were embodied in the cavity of β-CD, which was treated as AD-C$_{11}$im@2β-CD. With the increasing of AD-C$_{11}$im@2β-CD concentration, the appearance of the sample changed a lot, which was discussed in Phase diagrams of AD-C$_{11}$im/β-CD

Fig. 6 DLS (a) and TEM ((b) scale bar = 200 nm, (c) scale bar = 100 nm) results of 10 mM AD-C_{11}im@1β-CD.

system section. Consequently, the information on morphologies of these aggregates will be discussed in detail below.

To identify the morphology, transmission electron microstructure were observed in AD-C_{11}im@2β-CD system, shown in Fig. 8. The TEM observation results indicated that fibers, which were similar to Zukoski's studies,[36] emerged in AD-C_{11}im@2β-CD system when the concentration of AD-C_{11}im@2β-CD was 30 mM. The diameters of the fibers varied from 20 nm to 40 nm shown in Fig. 8a. Considering that the diameters of fibers were in nano-scale, the morphology of aggregates in AD-C_{11}im@2β-

CD system can be reported as nanofibers. Besides, these nanofibers were found to intertwine with each other shown in Fig. 8b and hence these nanofibers can be considered to be net-like nanofibers, which may be responsible for the non-transparent and viscoelastic appearance in Fig. 2d. The Small Angle X-Ray Scattering (SAXS) for AD-C_{11}im@2β-CD at 30 mM to receive the nanostructures morphology. As shown in Fig. S7,† It can be seen that there is no obvious Bragg diffraction peak in the SAXS spectrum. SAXS test implied that the structure of net-like nanofibers was disordered.
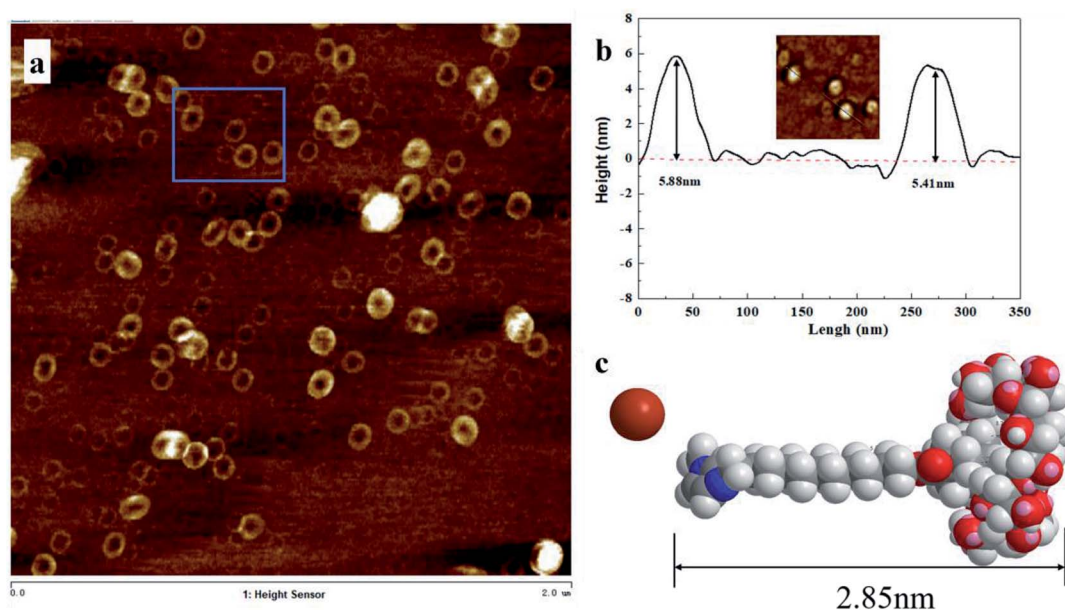
Fig. 7   (a) AFM image for aggregates from 10 mM AD-C$_{11}$im@1β-CD. (b) Sectional height profile of collapsed vesicles. (c) Molecular structure model of inclusion complex AD-C$_{11}$im @1β-CD.

With the increase of AD-C$_{11}$im concentration (above 35 mM), the solution did not flow even by inversion of the vial, indicating the formation of hydrogel. It is considered that gelation occurred because of cross-linked fibrillar networks. SEM is one of the most effective methods to study the morphology of hydrogel.[37,38] The SEM observation results in Fig. 9 showed that honeycomb structure caused by evaporation of water was appeared in the hydrogel, which meant the three-dimensional (3D) interconnected networks microstructure shaped.

FT-IR analysis of AD-C$_{11}$im@nβ-CD

It is generally known that hydrophobic interaction is mainly caused by alkyl chain. Hydrophobic interaction will not work during formation process of aggregates if alkyl chain is included in β-CD. According to ^{1}H–^{1}H 2D ROESY NMR of AD-C$_{11}$im@nβ-CD inclusions, the alkyl chain in the molecule was not encapsulated in a 1 : 1 system, but encapsulated in a 1 : 2 system. The results indicated that there were hydrophobic regions when the aggregates formed in AD-C$_{11}$im@1β-CD system and it was believed that there was almost no hydrophobic region when the aggregates shaped in AD-C$_{11}$im@2β-CD system. Accordingly, hydrophobic interaction was no longer the major driving force during forming process of aggregates in AD-C$_{11}$im@2β-CD system.

Compared with AD-C$_{11}$im itself, the hydrophobicity of AD-C$_{11}$im@nβ-CD inclusions decreased greatly owing to abundant

Fig. 8   TEM images of 30 mM AD-C$_{11}$im@2β-CD. (a) Scale bar = 200 nm. (b) Scale bar = 50 nm.
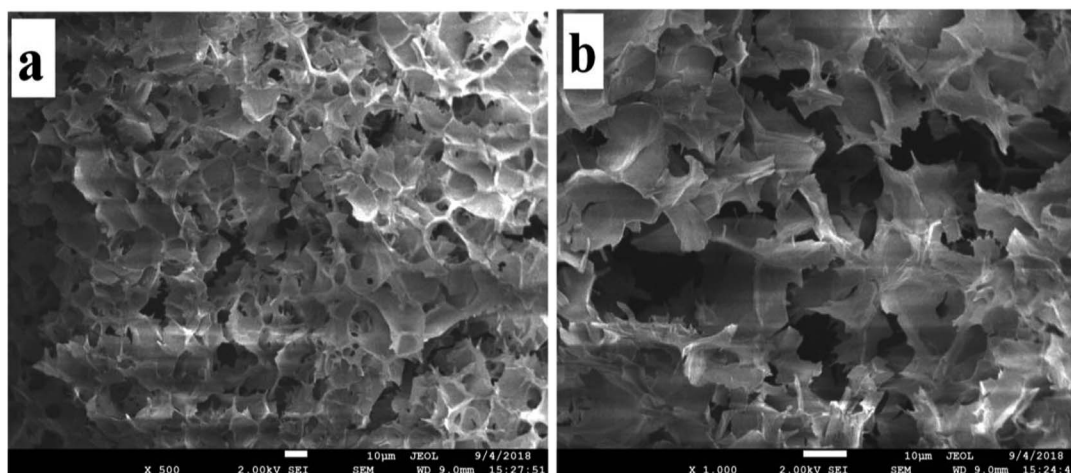
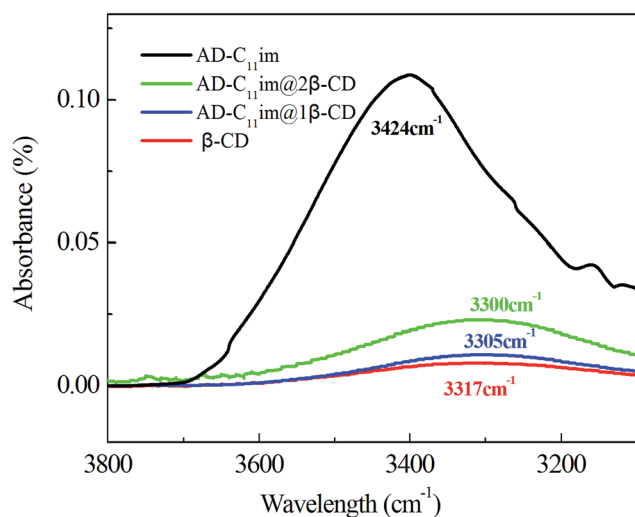**Fig. 9** SEM images of the hydrogel system with 50 mM AD-C_{11}im@2β-CD.

Fig. 10 FT-IR spectra for β-CD, AD-C_{11}im, AD-C_{11}im@1β-CD, AD-C_{11}im@2β-CD.

hydroxyl on the outer surface of β-CD. Thus, hydrogen bonding may play a key role. For this reason, the FT-IR spectra of β-CD, AD-C_{11}im@1β-CD and AD-C_{11}im@2β-CD samples were investigated and results were exhibited in Fig. 10 and Fig. S6.† It is

easy to see that the hydroxyl stretching vibration peak of pure CD was located at 3317 cm^{-1}. However, these of AD-C_{11}im@1β-CD and AD-C_{11}im@2β-CD samples were located at 3305 cm^{-1} and 3300 cm^{-1} separately. Both of them moved to the low wavenumber region. This revealed that a stronger hydrogen bond interaction was formed between β-CD during formation process of aggregates.[39]

In a word, it can be deduced that the self-assembly process should be driven mainly by hydrogen bonds between β-CD in AD-C_{11}im@2β-CD system. To prove this conclusion, a representative gel sample (AD-C_{11}im@2β-CD at 50 mM) was selected. From Fig. 11, it can be seen that the bluish hydrogel (Fig. 11a) started to flow when it was heated to 45 °C and then turned into transparent solution (Fig. 11c) when temperature was more than 80 °C. However, the gel was formed again after cooling. This indicates that hydrogen bonds between β-CD play a key role in AD-C_{11}im@2β-CD system.

Based on the above experimental data, AD-C_{11}im micelles transformed into other aggregate morphologies by adding β-CD are described in detail in Scheme 1. AD-C_{11}im, like traditional single chain surfactants, can be self-assembled into micelles in dilute aqueous solutions with hydrophilic imidazoles on the outer surface of micelles and hydrophobic adamantane in the core. However, the asymmetric bola-type amphiphilic molecule
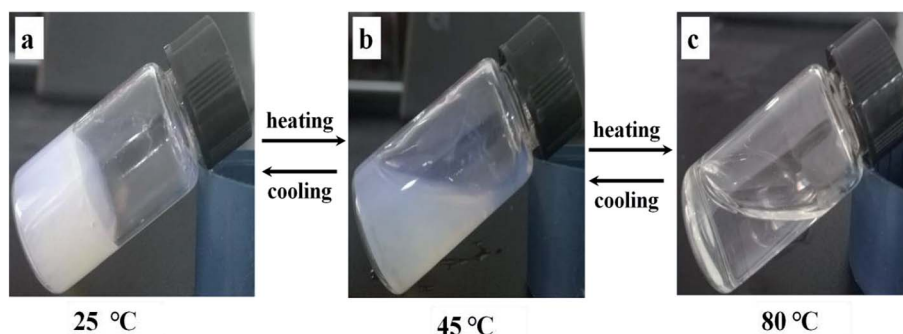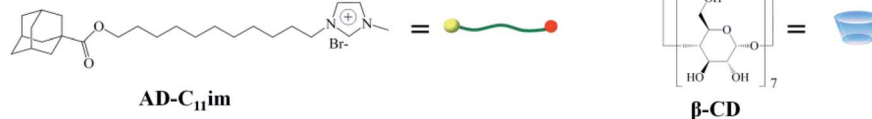

Fig. 11 Gel–sol transformation process of 50 mM AD-C_{11}im @2β-CD. (a) Hydrogel at 25 °C, (b) mesophase at about 45 °C, (c) clear solution at about 80 °C.

Scheme 1 Schematic diagram of the aggregation transformation of AD-C$_{11}$im induced by β-CD.

(AD-C$_{11}$im@1β-CD) was formed by the host–guest interaction between adamantane and β-CD after adding same molar amount of β-CD. Thus, hydrophobicity between alkane chains and hydrogen bonding between β-CD were the main driving forces, and asymmetric vesicles with the uncharged cyclodextrins in the outer wall and the charged pyridine group in the inner wall formed. When adding a double molar amount of β-CD, both adamantane and alkyl chain in AD-C$_{11}$im molecule were encapsulated by β-CD and the hydrophobic interaction was destroyed, which was no longer the main driving force. Then the building blocks (AD-C$_{11}$im@2β-CD inclusion) became unamphiphilic and driven by hydrogen bonding between β-CD to form net-like nanofiber. With the increase of AD-C$_{11}$im@2β-CD concentration, hydrogen bonding between β-CD strengthened and net-like nanofibers started to overlap and interweave. During the process, water molecules padded the spaces during the nanofibers.[40] As a result, the hydrogel with three-dimensional (3D) interconnected networks microstructure appeared.

Conclusions

All in all, a novel synthesized adamantane-based ionic liquid, AD-C$_{11}$im, was proved to have surface activities and can form micelles by electrical conductivity and DLS. What's more, the aggregation transformation of AD-C$_{11}$im by adding β-CD in different molars was investigated. Results showed that when the same amount β-CD was added in AD-C$_{11}$im aqueous solution, just adamantane was encapsulated by β-CD and the asymmetric bola-type amphiphilic molecule (AD-C$_{11}$im@1β-CD) was formed by the host–guest inclusion reaction between adamantane and β-CD. As a result, micelles were translated to vesicles, which were confirmed by DLS and TEM. Moreover, the vesicles were

proved to be single-layer structure by AFM. When adding a double molar amount of β-CD, ^{1}H–^{1}H 2D ROESY NMR results revealed that apart from adamantane, alkyl chain was also wrapped by β-CD. Driven by hydrogen bonding between β-CD, net-like nanofibers were found by TEM. With an increase in the AD-C$_{11}$im@2β-CD concentration up to 40 mM, net-like nanofibers became denser, started to intertwine with each other, and then the bluish hydrogel formed.

Conflicts of interest

There are no conflicts to declare.

Acknowledgements

Notes and references

1 J. J. Zhou, H. Sui, Z. D. Jia, Z. Q. Yang, L. He and X. G. Li, *RSC Adv.*, 2018, **8**(57), 32832–32864.

2 J. L. Shen, L. F. Song, X. Xin, D. Wu, S. B. Wang, R. Chen and G. Y. Xu, *Colloids Surf., A*, 2016, **509**, 512.

3 A. S. Amarasekara, *Chem. Rev.*, 2016, **116**, 6133.

4 M. Smiglak, J. M. Pringle, X. Lu, L. Han, S. Zhang, H. Gao, D. R. MacFarlane and R. D. Rogers, *Chem. Commun.*, 2014, **50**, 9228.

5 D. R. MacFarlane, N. Tachikawa, M. Forsyth, J. M. Pringle, P. C. Howlett, G. D. Elliott, J. H. Davis Jr, M. Watanabe, P. Simon and C. A. Angell, *Energy Environ. Sci.*, 2014, **7**, 232.

6 E. D. Bates, R. D. Mayton, I. Ntai and J. H. Davis, *J. Am. Chem. Soc.*, 2002, **124**, 926.

7 S. Pandey, *Anal. Chim. Acta*, 2006, **556**, 38.

8 Y. T. Kang, K. Liu and X. Zhang, *Langmuir*, 2014, **30**, 5989.

9 T. Sun, L. Shu, J. Shen, C. H. Ruan, Z. F. Zhao and C. Jiang, *RSC Adv.*, 2016, **6**, 52189.

10 N. Sharma and A. Baldi, *Drug Delivery*, 2016, **23**, 729.

11 S. Amajjahe and H. Ritter, *Macromolecules*, 2008, **41**, 3250.

12 Y. A. Gao, Z. H. Li, J. M. Du, B. X. Han, G. Z. Li, W. G. Hou, D. Shen, L. Q. Zheng and G. Y. Zhang, *Chem. –Eur. J.*, 2005, **11**, 5875.

13 Y. A. Gao, X. Zhao, B. Dong, L. Zheng, N. Li and S. Zhang, *J. Phys. Chem. B*, 2006, **110**, 8576.

14 L. Leclercq and A. R. Schmitzer, *J. Phys. Org. Chem.*, 2009, **22**, 91.

15 R. Ghosh, D. Ekka, B. Rajbanshi, A. Yasmin and M. N. Roy, *Colloids Surf., A*, 2018, **548**, 206.

16 Y. F. He, Q. D. Chen, C. Xu, J. J. Zhang and X. H. Shen, *J. Phys. Chem. B*, 2009, **113**, 231.

17 J. J. Zhang and X. H. Shen, *J. Phys. Chem. B*, 2013, **117**, 1451.

18 X. Zhong, J. W. Guo, L. Z. Feng, X. J. Xu and D. Y. Zhu, *Colloids Surf., A*, 2014, **441**, 572.

19 J. Wang, M. H. Yao, Q. T. Li, S. J. Yi and X. Chen, *Soft Matter*, 2016, **12**, 9641.

20 X. Zhong, C. X. Hu, X. W. Yan, X. Liu and D. J. Zhu, *J. Mol. Liq.*, 2018, **272**, 209.

21 I. Béjaoui, M. Baâzaoui, Y. Chevalier, N. Amdouni, R. Kalfat and S. Hbaieb, *J. Inclusion Phenom. Macrocyclic Chem.*, 2016, **86**, 79.

22 V. I. Martín, P. López-Cornejo, M. López-López, D. Blanco-Arévalo, A. J. Moreno-Vargas, M. Angulo, A. Laschewsky and M. L. Moyá, *Arabian J. Chem.*, 2018, DOI: 10.1016/j.arabjc.2018.04.015.

23 Y. Deng, Y. Pang, Y. Guo, Y. Ren, F. Wang, X. Liao and B. Yang, *J. Mol. Struct.*, 2016, **1118**, 307.

24 J. J. Jiao, B. Dong, H. N. Zhang, Y. Y. Zhao, X. Q. Wang, R. Wang and L. Yu, *J. Phys. Chem. B*, 2012, **116**, 958.

25 T. Singh and A. Kumar, *J. Phys. Chem. B*, 2007, **111**, 7843.

26 A. J. Valente and O. Söderman, *Adv. Colloid Interface Sci.*, 2014, **205**, 156.

27 L. X. Jiang, Y. Yan and J. B. Huang, *Adv. Colloid Interface Sci.*, 2011, **169**, 13.

28 H. C. Zhang, J. Shen, Z. N. Liu, A. Y. Hao, Y. Bai and W. An, *Supramol. Chem.*, 2010, **22**, 297.

29 H. Jia, X. Leng, D. Q. Zhang, P. Lian, Y. P. Liang, H. Y. Wu, P. Huang, J. P. Liu and H. T. Zhou, *J. Mol. Liq.*, 2018, **255**, 370.

30 Z. L. Zhai, L. Lei, J. Y. Song, B. L. Song, X. M. Pei and Z. G. Cui, *Soft Matter*, 2016, **12**, 2715.

31 H. L. Zhao, X. Song, H. Aslan, B. Liu, J. G. Wang, L. Wang, F. Besenbacher and M. D. Dong, *Phys. Chem. Chem. Phys.*, 2016, **18**, 14168.

32 D. S. Guo, K. Wang, Y. X. Wang and Y. Liu, *J. Am. Chem. Soc.*, 2012, **134**, 10244.

33 G. T. Wang, Y. T. Kang, B. H. Tang and X. Zhang, *Langmuir*, 2014, **31**, 120.

34 S. Landsmann, M. Luka and S. Polarz, *Nat. Commun.*, 2012, **3**, 1299.

35 A. Sikder, A. Das and S. Ghosh, *Angew. Chem.*, 2015, **127**, 6859.

36 M. Zhang and C. F. Zukoski, *Langmuir*, 2014, **30**, 7540.

37 S. Y. Li, P. Y. Xing, Y. H. Hou, J. S. Yang, X. Z. Yang, B. Wang and A. Y. Hao, *J. Mol. Liq.*, 2013, **188**, 74.

38 X. Z. Hu and C. J. Zou, *Colloids Surf., A*, 2017, **529**, 571.

39 C. C. Zhou, J. B. Huang and Y. Yan, *Soft Matter*, 2016, **12**, 1579.

40 T. Vermonden, R. Censi and W. E. Hennink, *Chem. Rev.*, 2012, **112**, 2853.